Long-Term GPS Carrier-Phase Time Transfer Noise: A Study based on Seven GPS Receivers at NIST

Jian Yao, and Judah Levine
Time and Frequency Division and JILA, National Institute of Standards and Technology and University of Colorado, Boulder, Colorado 80305, USA
E-mail: jian.yao@nist.gov

***Abstract*—This paper reports a preliminary study of the long-term GPS carrier-phase time transfer noise, based on seven NIST GPS receivers. We find that the difference in carrier-phase time-transfer result using any two GPS receivers over 100 days can change by ~ 0.5 ns (peak-to-peak) in most cases and by ~ 1.3 ns (peak-to-peak) in some extreme cases. This suggests that a more frequent GPS calibration is needed to achieve sub-nanosecond GPS timing accuracy.**

Keywords—GPS, Carrier-Phase Time Transfer, Long-Term Noise, Revised RINEX-Shift (RRS) Algorithm

I. INTRODUCTION

Global Positioning System (GPS) carrier-phase (CP) time transfer is a widely accepted high-precision time transfer method. This method provides much lower short-term (< 0.5 day) noise than other time transfer methods, such as GPS code-based common-view (CV) time transfer and Two Way Satellite Time and Frequency Transfer (TWSTFT) [1-3].

A recent study showed that the relative change between GPS CP time transfer and TWSTFT can be as large as 6-7 ns over a few years [4]. However, we do not know whether the relative change comes from GPS CP, or TWSTFT, or both. Thus, we want to know the long-term (> 30 days) uncertainty in both GPS CP and TWSTFT.

This paper focuses on the long-term (> 30 days) uncertainty in GPS CP time transfer, based on a zero-baseline study. As we know, the short-term noise of GPS CP time transfer increases as the baseline increases, because the noise from troposphere, ionosphere, and GPS satellites can no longer be exactly cancelled out. However, these types of noise can be averaged down and becomes negligible after a few days, if we apply proper models or some real measurements/estimations which is done in the GPS carrier-phase time transfer processing. Thus, the long-term uncertainty in GPS CP time transfer should be independent of the length of a baseline, or at most have a small dependence. Because of this, the zero-baseline study in this paper represents the long-term uncertainty in GPS CP time transfer, for any baseline. Section II shows the experimental setup and the data processing. Section III presents the CP time transfer results using all NIST receivers. We will see that different GPS receivers give different time-transfer results. The difference in time transfer can be as large as ~ 1.3 ns, for an extreme case. This long-term uncertainty in GPS CP time transfer proposes a challenge to the GPS total-delay calibration, if sub-nanosecond GPS timing accuracy is needed. Section IV concludes the paper.

II. EXPERIMENTAL SETUP AND GPS DATA PROCESSING

At NIST, we had 7 GPS receivers running properly for most time of 2014. They were *NIS2*, *NISA*, *NISS*, *NIST*, *NISW*, *NISX*, and *NISY*. All of them had the same reference time, i.e., UTC(NIST). *NISA*, *NISS*, and *NISW* were connected to the same antenna. The other four receivers were connected to four different antennas. The physical locations of all antennas were illustrated by Figure 1. The maximum distance between two antennas was approximately 130 m. We would like to mention that the seven GPS receivers and their antennas were from a few different manufacturers (see Table 1).

In this paper, we achieve the GPS carrier-phase time transfer via three different data-processing methods: NRCan Precise Point Positioning (PPP) 1-day method, NRCan PPP 30-days method, and Revised RINEX-Shift (RRS) method. The NRCan PPP software package is developed by Natural Resource Canada [5]. Originally, it can only process the GPS data for a single day. We call it "NRCan PPP 1-day method" here. Similar to other PPP software (such as Atomium PPP [6] and Novatel GrafNav PPP), the NRCan PPP 1-day method has the problem of day boundary discontinuity in its time solution [7]. To mitigate this problem, people extend the length of data processing from 1 day to multi-days (e.g., 30 days) [8]. In this way, we no longer have the day boundary discontinuity. Instead, we have a discontinuity between two 30-days data batches. We call this method "NRCan PPP 30-days method". The RRS method, invented in 2014, completely solves the problem of day boundary discontinuity [9-10]. Because of this, this method provides a continuous GPS carrier-phase time transfer result. Thus it is good to monitor the small change in time transfer for a long time. The performance of the RRS method can be found in [9, 11]. We should mention that the short-term performance of the original RRS was worse than that of NRCan PPP as indicated in [11]. A recent update of this method shows that its short-term (< 3 hours) stability is comparable to NRCan PPP. This will also be shown later in this paper. Since RRS is a relatively new method, we provide the NRCan solutions in this paper, to be more convincing.

The three methods have the same settings. The cutoff elevation is 10 degrees. The mapping function of tropospheric delay is "global mapping function (GMF)". We apply the same ocean tide loading to all NIST receivers. We only use GPS

978-1-5090-2091-1/16/$31.00 ©2016 IEEE

data, and do not use Glonass, Beidou, or Galileo data. The International GNSS Service (IGS) final products (SP3 and CLK) are used as the input files.

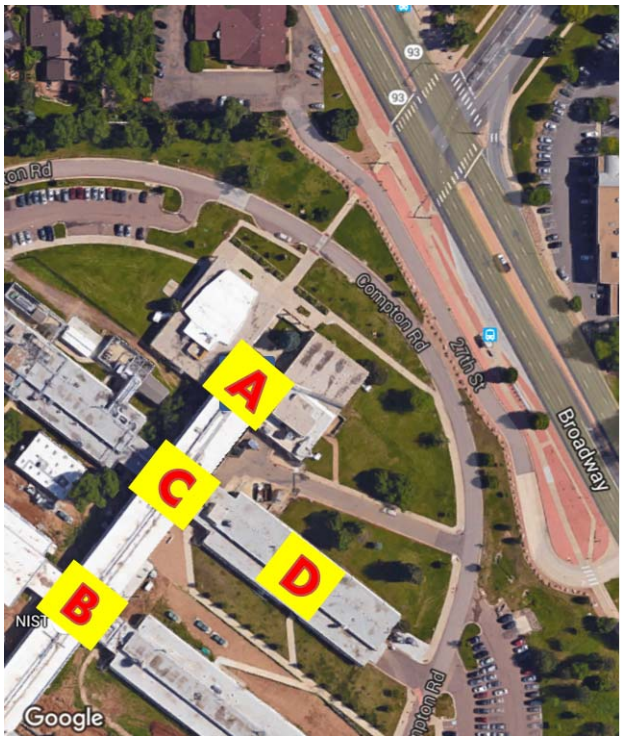

Figure 1. Google map of NIST. The antennas of the *NIS2*, *NISX*, and *NISY* receivers were located in Zone A. The antennas of the *NISA*, *NISS*, *NIST*, and *NISW* receivers were located in Zone B. *NISA*, *NISS*, and *NISW* shared the same antenna. Zone C is a penthouse, and Zone D is a building.

Table 1. NIST receiver models and corresponding antenna models

Receiver Name	Receiver Model	Antenna Model
NIS2	Novatel OEM5	NOV GNSS 750 (ChokeRing)
NISA	Ashtech Z12T	Ash701945G_M (ChokeRing)
NISS	SEPT Polarx3ETR	Ash701945G_M (ChokeRing)
NIST	Novatel OEM4	NOV 702 (Pinwheel)
NISW	Novatel OEM5	Ash701945G_M (ChokeRing)
NISX	Novatel OEM4	NOV 702 (Pinwheel)
NISY	Novatel OEM5	NOV GNSS 750 (ChokeRing)

III. Results and Discussions

Here, we run the RRS data processing for all seven NIST receivers, for MJD 56925.000 – 57017.999 (i.e., Sep. 25, 2014 – Dec. 26, 2014). The result is shown by Figure 2. We shift all curves so that they are 0 at 56925.000, for a better comparison. For the *NISS* receiver, since it only has data during 56932.000 – 57017.999, we shift its time-transfer result (black curve) to be the same as the *NISY*'s result (cyan curve) at 56932.000. From Figure 2, we can see that the time differences between UTC(NIST) and IGS final time scale via all receivers are almost the same. All curves have similar trends. However, there is still some difference among curves. Figure 3 is enlarged from Figure 2. This shows more details at around MJD 56955 (i.e., 30 days from the beginning). We can see that the maximum time-transfer difference between two receivers is about 0.4 ns. Similar to Figure 3, Figure 4 shows more details at around MJD 57017, which is 92 days from the beginning. The maximum time-transfer difference between two receivers is about 0.7 ns. This indicates that even if we have an ideal calibration on MJD 56925, the absolute GPS timing error can be as large as 0.7 ns after ~ 90 days.

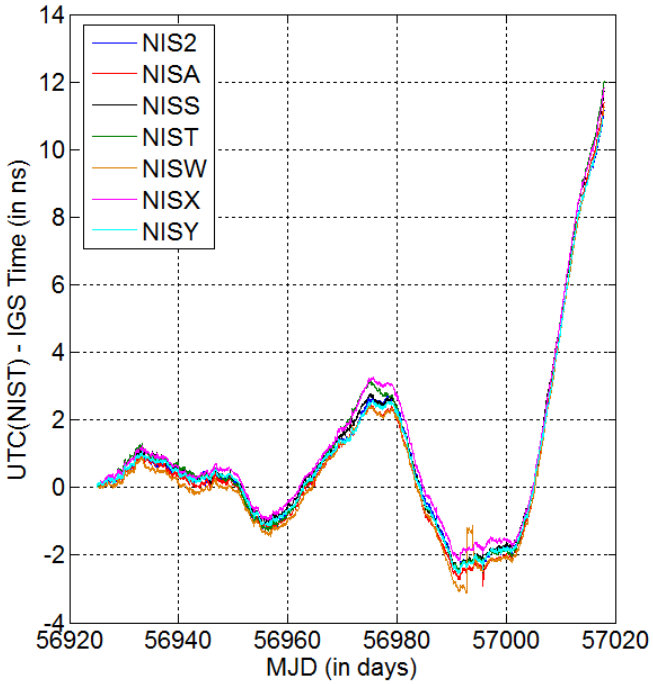

Figure 2. Time difference between UTC(NIST) and IGS final time scale during 56925.000 – 57017.999, using 7 NIST receivers. The curves are shifted to 0 ns at the epoch of MJD 56925.000, for a better comparison. Note, the *NISS* receiver only has data during 56932.000 – 57017.999, so we shift it to be the same as *NISY* at MJD 56932.000.

Another thing we want to address is that the curves in Figure 2 do not diverge from each other linearly as time goes. In other words, there is no guarantee that one curve is above another curve all the time. As an example, at the beginning (i.e., MJD 56925.0), both *NISY* and *NISA* are 0. After 29.5 days (see Figure 3), *NISY* is above *NISA*. However, after 91.5 days

(see Figure 4), *NISY* is below *NISA*. This means, the time delay for a receiver is rather a random number. There is no linear change of the time delay.

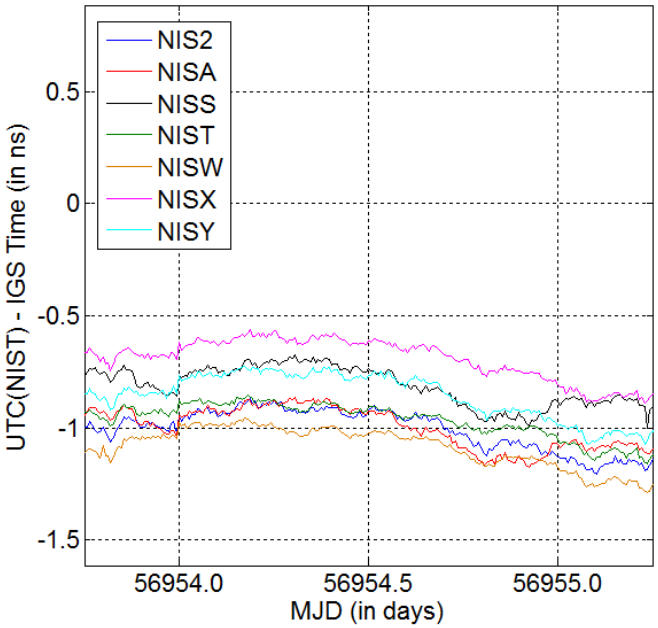

Figure 3. Time difference between UTC(NIST) and IGS final time scale around MJD 56955.000, using 7 NIST receivers. This figure is enlarged from Figure 2.

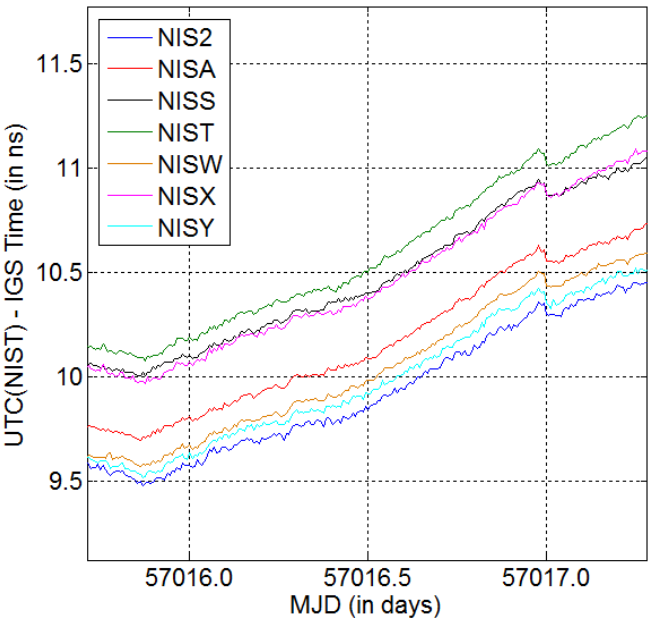

Figure 4. Time difference between UTC(NIST) and IGS final time scale around MJD 57017.000, using 7 NIST receivers. This figure is enlarged from Figure 2.

To see more details about the relative time change between two receivers, we do the time difference between two receivers. The time difference between two receivers sharing the same reference time is called "common-clock difference (CCD)" in some papers [12-13]. In principle, the time difference between two NIST receivers should be a constant. However, in practice, different receivers give slightly different time-transfer results, as indicated in Figure 2. This leads to a non-constant time difference. As an example, we do the time difference between *NISX* (the magenta curve in Figure 2) and *NISY* (the cyan curve in Figure 2). The result is shown by Figure 5. We can see that the time difference can vary by up to ~ 0.75 ns for the whole 93 days.

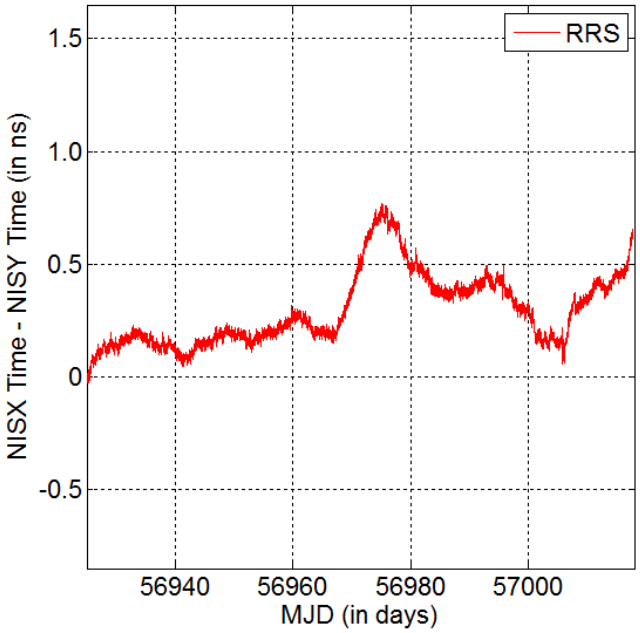

Figure 5. Time difference between the *NISX* time (i.e., the UTC(NIST) via the *NISX* receiver) and the *NISY* time (i.e., the UTC(NIST) via the *NISY* receiver) during MJD 56925.000 – 57017.999, using the RRS method.

At this point, people may wonder if RRS is working properly. After all, RRS is a relatively new technique. To make our above result more convincing, we compare the RRS result with the NRCan PPP results. Figure 6 is the same as Figure 5, except that it also has the NRCan PPP 1 day result. It is very hard to identify the pattern in the time difference between *NISX* and *NISY* based on the blue curve in Figure 6, because the day boundary discontinuity occurs too often and smears the actual features. Figure 7 compares RRS with NRCan PPP 30 days. We can see that NRCan PPP 30 days has similar patterns to RRS. For example, both curves have a peak at ~ MJD 56975. Both have a small dent at ~ MJD 56942. This verifies that RRS is doing things right. The advantage of RRS over NRCan PPP 30 days is that it removes the jumps at the 30-days boundary (i.e., MJD 56928.0, 56958.0, and 56988.0). Because of this, the frequency stability of RRS is slightly better than that of NRCan PPP 30 days at 0.25 – 3 days (see Figure 8). We would like to emphasize that the short-term stability of RRS is the same as that of NRCan PPP 30 days, after some updates in RRS. In summary, RRS allows us to see the relative time change between two receivers more clearly.

We find that the relative time change between *NISX* and *NISY* shown by Figure 5 is common. Most of other links have a

similar change of 0.5 – 0.8 ns (peak-to-peak) during the 93 days. The best link we find is the "*NIS2 – NISY*" link (Figure 9). We can see that the peak-to-peak change is only ~ 0.3 ns. Notice that both *NIS2* and *NISY* use the same receiver model and the same antenna model (see Table 1). This result gives the best carrier-phase time transfer we can achieve for a long term. It also sets the fundamental limit in the GPS calibration.

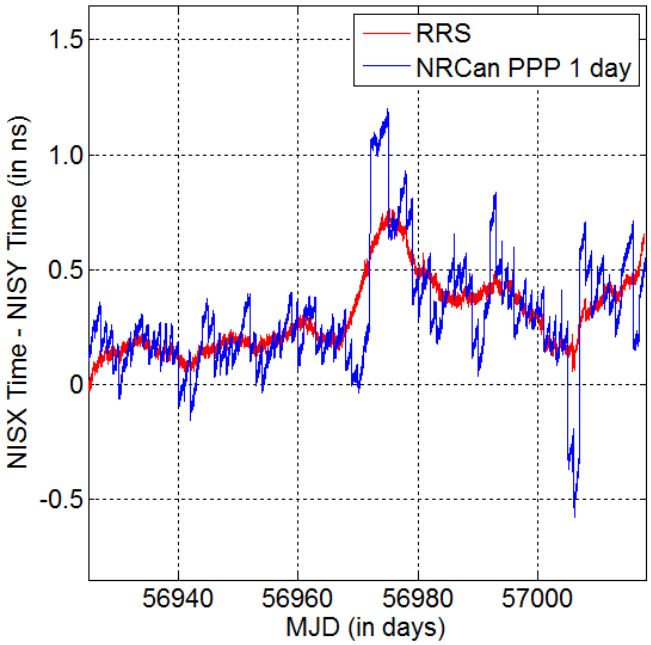

Figure 6. Comparison of the RRS method and the NRCan PPP 1 day method.

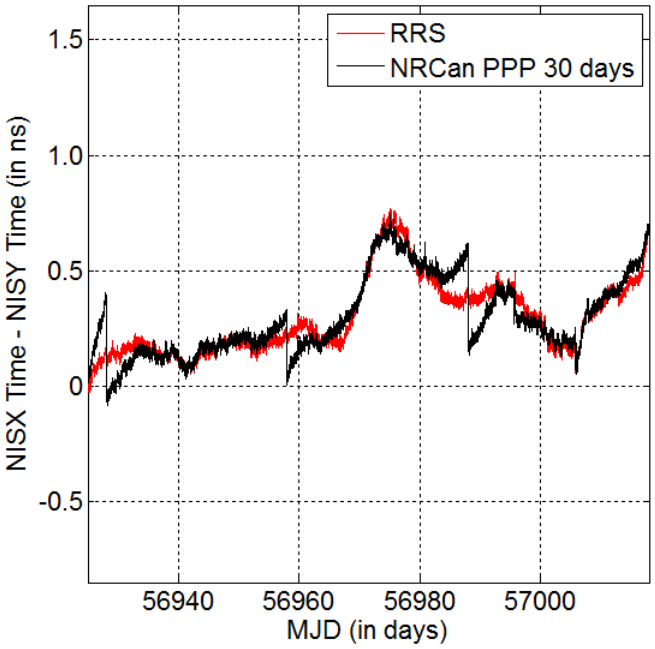

Figure 7. Comparison of the RRS method and the NRCan PPP 30 day method.

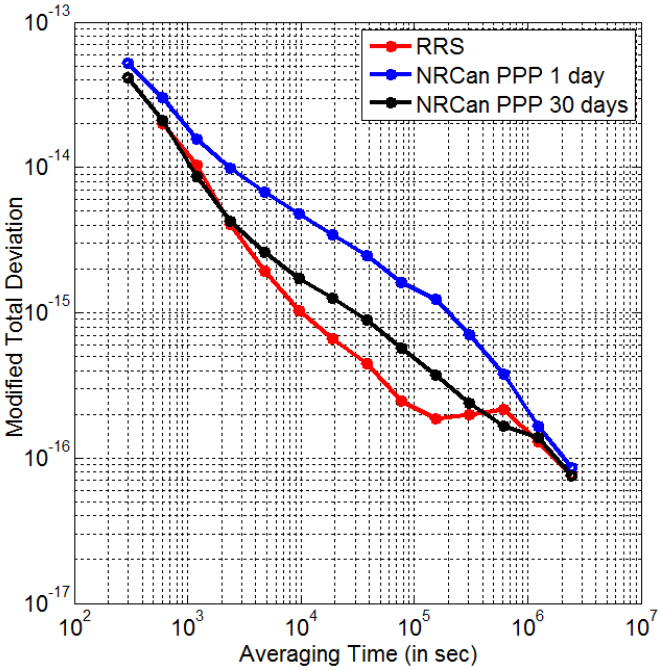

Figure 8. Frequency stability of RRS, NRCan PPP 1 day, and NRCan PPP 30 days, for the double difference between *NISX* and *NISY* during 56925.000 – 57017.999.

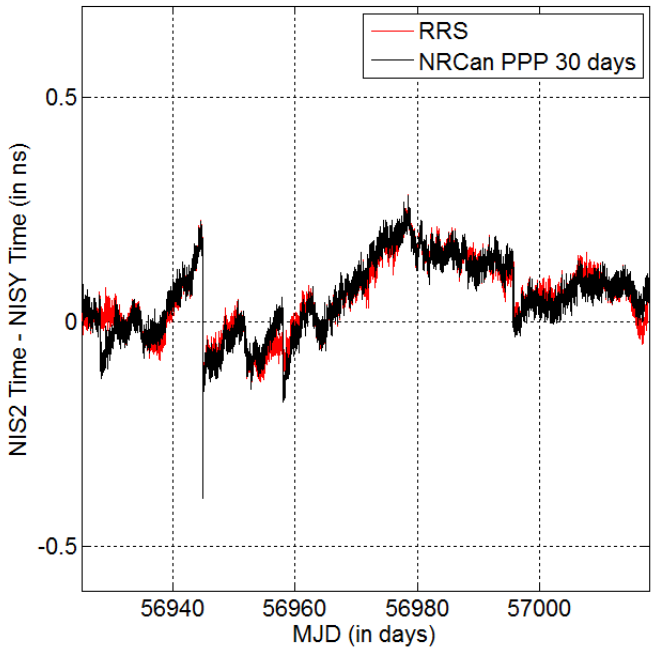

Figure 9. Time difference between the *NIS2* time and the *NISY* time during MJD 56925.000 – 57017.999, using both the RRS method and the NRCan PPP 30 days method. Note, the jump on around MJD 56945 is due to missing GPS data. We have not repaired this data anomaly in RRS because of limited time. A later report will repair this anomaly.

Last, we explore the maximum long-term error in carrier-phase time transfer. Figure 10 shows an extreme case. The time difference between *NIST* and *NISY* varies by as large as ~ 1.3 ns, during MJD 56690 - 56764. Especially, the large change occurs mainly during MJD 56690 – 56705. This proposes a challenge to the GPS calibration, if we want to achieve sub-nanosecond accuracy.

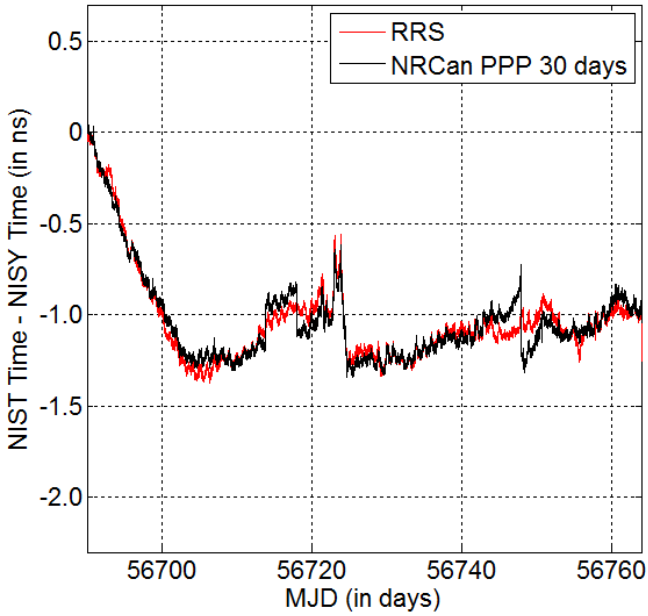

Figure 10. Time difference between the *NIST* time and the *NISY* time during MJD 56690.000 – 56763.999, using both the RRS method and the NRCan PPP 30 days method.

IV. Conclusions

In summary, the CP time-transfer result using one receiver can typically vary from that using another receiver by approximately ~0.6 ns (peak-to-peak), during 100 days. For an extreme case, the time difference between two common-clock receivers can vary by as large as ~ 1.3 ns during 100 days. This suggests that a more frequent calibration or a reference-delay monitoring system is needed to achieve sub-nanosecond GPS timing accuracy.

Acknowledgments

The authors thank Francois Lahaye for sharing the NRCan PPP software. We also thank Marc Weiss for installing and maintaining the NIST receivers in 2014. In addition, we thank Neil Ashby and Biju Patla for their comments. IGS is gratefully acknowledged for providing GPS tracking data, station coordinates, and satellite ephemerides.

Disclaimer

Product names and model numbers of the equipment are included for reference only. No endorsement or criticism is implied.

References

[1] Z. Jiang, R. Dach, G. Petit, T. Schildknecht, and U. Hugentobler, "Comparison and combination of TAI time links with continuous GPS carrier phase results," Proc. 20th EFTF Meeting, pp. 440-447, 2006.

[2] S. Y. Lin, W. H. Tseng, H. T. Lin, K. M. Feng, and D. Piester, "The comparison between TWSTFT and GPS time transfer result of PTB-TL link," Proc. 2009 IEEE IFCS-EFTF Meeting, pp. 1203-1205, 2009.

[3] V. Zhang, and T. E. Parker, "A study of the diurnal in the transatlantic TWSTFT difference," 2013 Asia-Pacific time and frequency workshop, 2013.

[4] V. Zhang, T. E. Parker, and J Yao, "Long-term uncertainty in time transfer using GPS and TWSTFT techniques," Proc. 2015 IEEE IFCS-EFTF Meeting, pp. 723-727, 2015.

[5] J. Kouba and P. Heroux, "Precise point positioning using IGS orbit and clock products," GPS Solutions, vol. 5, pp. 12–28, 2001.

[6] Q. Baire, C. Bruyninx, P. Defraigne, and J. Legrand, "Precise point positioning with Atomium using IGS orbit and clock products: first results," Bulletin of Geodesy and Geomatics, vol. 69, n. 2-3, pp. 396-404, 2010.

[7] J. Yao, Section 2.6 of "Continuous GPS carrier-phase time transfer," PhD Thesis, University of Colorado at Boulder, 2014.

[8] G. Petit, "The TAIPPP pilot experiment," Proc. 2009 IFCS-EFTF Joint Conference, pp. 116-119, 2009.

[9] J. Yao, and J. Levine, "An improvement of RINEX-Shift algorithm for continuous GPS carrier-phase time transfer," Proc. 27th ION GNSS+ 2014 Conference, pp. 1253–1260, 2014.

[10] J. Yao and J. Levine, "A new algorithm to eliminate GPS carrier-phase time transfer boundary discontinuity," Proc. 45th Annual Precise Time and Time Interval (PTTI) Systems and Applications Meeting, pp. 292–303, 2013.

[11] J. Yao, I. Skakun, Z. Jiang, and J. Levine, "A detailed comparison of two continuous GPS carrier-phase time transfer techniques," Metrologia, 52, pp. 666-676, 2015.

[12] Z. Jiang, "Final report of the BIPM pilot study on UTC time link calibration," Proc. 47th Annual Precise Time and Time Interval (PTTI) Systems and Applications Meeting, pp. 20-26, 2016.

[13] Z. Jiang, D. Matsakis, V. Zhang, H. Esteban, D. Piester, S. Y. Lin, and E. Dierikx, "A TWSTFT calibration guideline and the use of a GPS calibrator for UTC TWSTFT link calibrations," Proc. 47th Annual Precise Time and Time Interval (PTTI) Systems and Applications Meeting, pp. 231-242, 2016.